Maturity assessment of 'Rojo Brillante' persimmon by Hyperspectral Imaging

S. Munera[a*], J. Blasco[a], S. Cubero[a], C. Besada[b], A. Salvador[b], P. Talens[c], N. Aleixos[d]

[a] Centro de Agroingeniería. Instituto Valenciano de Investigaciones Agrarias (IVIA). Ctra. Moncada-Náquera Km 4.5, 46113, Moncada, Valencia (Spain)

[b] Centro de Tecnología Postcosecha. Instituto Valenciano de Investigaciones Agrarias (IVIA). Ctra. Moncada-Náquera Km 4.5, 46113, Moncada, Valencia (Spain)

[c] Departamento de Tecnología de Alimentos. Universitat Politècnica de València. Camino de Vera, s/n, 46022 Valencia (Spain)

[d] Departamento de Ingeniería Grafica. Universitat Politècnica de València. Camino de Vera, s/n, 46022 Valencia (Spain)

* Corresponding author. Email: munera_san@gva.es

Abstract

Persimmon cv. 'Rojo Brillante' is an astringent cultivar highly appreciated by consumers due to its good aspect, high size, sweetness and absence of seeds. However, this cultivar is very astringent and the fruit cannot be consumed until a high degree of overripeness with takes long time and makes the fruit difficult to handle. A method based on exposing fruit to high CO_2 concentrations was recently developed to eliminate quickly the astringency preserving the firmness; however, the adequate duration of this treatment depends mostly on the maturity at harvest. Therefore the aim of this work was to investigate a non-destructive and reliable method based on hyperspectral imaging to assess the maturity of persimmon cv 'Rojo Brillante' before deastringency treatments. For this purpose, 150 persimmon fruits were harvested at three different stages of commercial maturity and flesh firmness was determined after the image acquisition. Hyperspectral images of each fruit were taken using a hyperspectral system based on two liquid crystal tuneable filters, sensitive in the spectral range 420-1080 nm. Partial Least Square-Discriminant Analysis (PLS-DA) was used on the hyperspectral images to select optimal wavelengths and classify persimmon fruits by maturity. The results achieved 90.1% of correct classification using six selected wavelengths. Additionally, flesh firmness was predicted by using partial least square regression (PLS-R) and the selected wavelengths. A R^2 of 0.80 and a square error of prediction (SE_P) of 4.34 N were obtained. All of these results were considered as good for a non-invasive maturity assessment technique of 'Rojo Brillante' persimmon.

Keywords: fruit, internal quality, classification, prediction, computer vision

1. Introduction

Persimmon cv. 'Rojo Brillante' is an astringent cultivar mostly located in the region of Ribera del Xuquer (Valencia, Spain) which is very appreciated by consumers because its good aspect, big size, sweetness and absence of seeds. Naturally, this cultivar is astringent and cannot be consumed until a certain degree of overripeness. This has been traditionally a handicap for the commercialization of this fruit since once the fruit loss the astringency by overripen, the fruit is soft and losses the firmness so that it melts being difficult to handle. The demand of "crispy texture" persimmons has importantly increased in the last years while the market of soft fruit is coming to be reduced. Thus, the application of deastringency treatment applying high CO_2 concentration has become a habitual practice to commercialize astringent cultivars since it allows the removal of astringency while maintaining high flesh firmness (Salvador et al., 2007; Besada et al., 2010). This treatment for a period between 24-36h has been utilized to create a new product which is commercialized under the commercial name of Persimon® which is a non-astringent fruit with a firm and crispy texture. However, the duration of these treatments depends mostly of the firmness at harvest, since it has been suggested that the CO_2 diffusion across the parenchyma is reduced as the fruit loss firmness (Salvador et al., 2008).

Nowadays, the maturity index for harvesting 'Rojo Brillante' persimmons is the visual evaluation of external colour, since the changes from green to orange-red during fruit maturation have been observed to be closely related to the gradual decline of fruit firmness as well as to other internal physicochemical changes (Salvador et al., 2007). Hyperspectral imaging can offer the possibility to study the fruit in the regions where the human eye is unable to operate, such as ultraviolet (UV) or near infrared (NIR) regions (Lorente et al., 2012). This is a powerful inspection tool which has increased considerably in recent years to assess fruit maturity (Lleó et al., 2011; Rajkumar et al., 2012; Schmilovitch et al., 2014) but also to detect defects, damages or contaminants (Gaston et al., 2010; Lü et al., 2011; Yang et al., 2012; Baranowski et al., 2013; Lee et al., 2014; Teena et al., 2014; Zhang et al., 2015). The breadth of their applications lies in the fact that hyperspectral systems provide substantial information about the nature and attributes of the objects present in a scene by the pixel spectrum.

Therefore, the aim of this work was to investigate a non-destructive and reliable method based on hyperspectral imaging to assess the maturity of persimmon cv. 'Rojo Brillante' looking to deastringency treatments.

2. Materials and Methods

2.1. Plant material and physiological characterization

In this study, 150 persimmon fruit (*Diospyros kaki* Thunb. cv. 'Rojo Brillante') were harvested in L´Alcudia (Valencia, Spain) at three different moments of commercial season during November and December 2014 to obtain three different stages of maturity (M1, M2 and M3).

The maturity index used to select the fruits was a visual observation of the external colour of the fruit (Salvador et al., 2007). To determine the skin colour, a colourimeter (CR-300, Konica Minolta Inc, Tokyo, Japan), with a Standard Illuminant C, Standard Observer 2° and a field of view of 8-mm diameter was used. HunterLab colour coordinates were obtained by the average of both sides and expressed as colour index (CI) (Jiménez-Cuesta et al., 1981) (Eq 1).

$$CI = \frac{1000\,a}{Lb} \qquad (1)$$

Flesh firmness was evaluated after image acquisition by means of a universal testing machine (4301, Instron Engineering Corp., MA, USA) with an 8 mm flat plunger was used. During the test, the crosshead speed was 10 mm/min and the force increased until it drastically decreased; it is in this moment that the flesh is broken and the maximum peak force is registered. Results were expressed as the load in Newton (N) required for breaking the flesh of the fruit on opposite sides after peel removal.

Analysis of variance (ANOVA) and Tukey multiple range test (Statgraphics Centurion XVI - Statpoint Technologies Inc., Virginia, USA) were used to show the effects of maturity on flesh firmness and external colour (Figure 1).
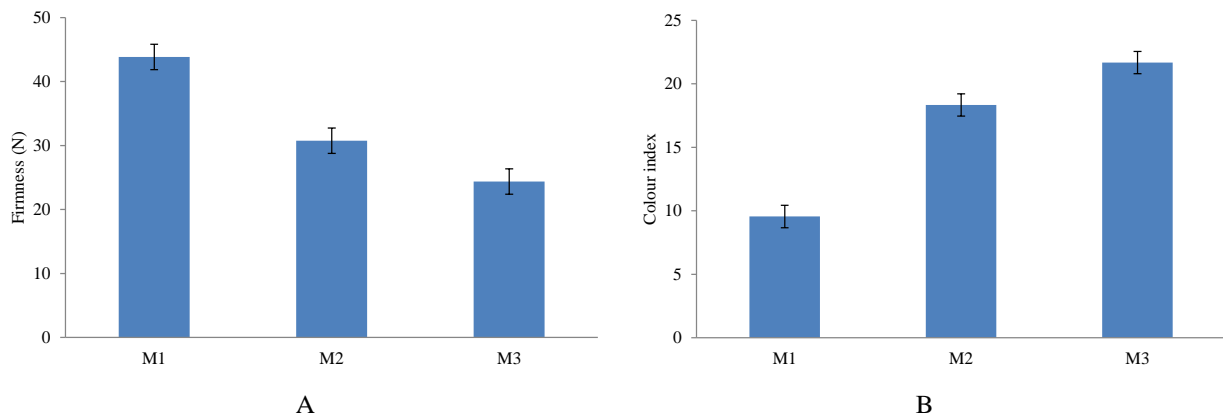

Figure 1. Flesh firmness (A) and external colour (B) characterization of 'Rojo Brillante' persimmon fruits. Vertical bars represent Tukey HSD intervals (P = 0.05).

2.2. Image acquisition and data analysis

Hyperspectral system composed by an industrial camera (CoolSNAP ES, Photometrics, AZ, USA), coupled to two liquid crystal tuneable filter (LCTF) (Varispec VIS-07 and NIR-07, Cambridge Research & Instrumentation, Inc., MA, USA), capable of acquiring images in the spectral range 420 nm - 1070 nm was used for image acquisition. The system was configured to capture images of 1392 x 1040 pixels with a spatial resolution of 0.14 mm/pixel and a spectral resolution of 10 nm. The focus was adjusted on the central band of the acquisition interval (740 nm) and the images were captured using a lens capable of covering the whole spectral range without losing the focus. The integration time of each band was calibrated to capture the averaged gray level of a white reference target corresponding to 90 % of the dynamic range of the camera. The illumination system consisted of 12 halogen spotlights of 37 W each (Eurostar IR Halogen MR16. Ushio America, Inc., CA, USA) powered by direct current (12 V), that lit the scene indirectly by means of diffuse reflection inside a hemispherical dome where whole fruits were manually introduced. The inner surface of the aluminium dome was painted white in order to maximise its reflectivity (Figure 2).
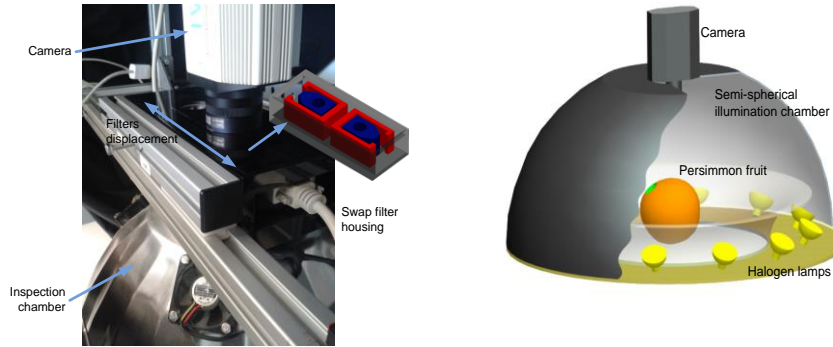
Figure 2. Hyperspectral imaging system.

One hyperspectral image, in reflectance mode, was captured of each fruit, forming a database of a total of 150 hyperspectral images in the working range 450-1020 nm. In each image, a representative region of interest (ROI) of the whole fruit surface, avoiding stem and dark borders, was selected (Figure 3). Later, all the images were corrected to obtain the relative value of the pixel in the position (x,y) of the monochromatic band λ. This correction was performed using equations by Gat (2000) as outlined in (2):

$$\rho_{xy}(x,y,\lambda) = \frac{R^{abs}}{R^{abs}_{white}} = \rho^{Ref}(\lambda)\frac{R(x,y,\lambda)-R_{black}\ (x,y,\lambda)}{R_{white}\ (x,y,\lambda)-R_{black}\ (x,y,\lambda)} \qquad (2)$$

Where $\rho^{Ref}(\lambda)$ is the standard reflectance of the white reference (99%), $R(x,y,\lambda)$ is the reflectance of the fruit captured by the CCD, $R_{white}(x,y,\lambda)$ is the white reflectance captured by CCD and $R_{black}(x,y,\lambda)$ the reflectance captured by the CCD avoiding any light source to quantify the electronic noise of the CCD.

Then, the average spectrum of the pixels in the ROI was calculated and considered as the fruit sample. These processes were performed using customised software developed at IVIA. In order to remove possible scatter effects from original spectral data, Standard Normal Variate (SNV) was applied.

Finally, Partial Least Square Discriminant Analysis (PLS-DA) and Partial Least Square Regression (PLS-R) were applied to classify the fruit in each stage of maturity and to predict flesh firmness, respectively. Both models were built using the spectra of 150 fruits and were divided in two sets: 66% of the fruits were included in the calibration set and the rest of the samples were considered as classification/prediction set. All of them were randomly chosen to select the same number of fruit of each stage of maturity. In the PLS-DA model, the samples of each stage of maturity were codified with dummy codes: M1 = (1 0 0), M2 = (0 1 0) and M3 = (0 0 1). In the case of PLS-R, samples were correlated with firmness data. Models were internally validated using the full-cross validation technique. The software used in this case was The Unscrambler X 10.1 (CAMO Software, Oslo, Norway).
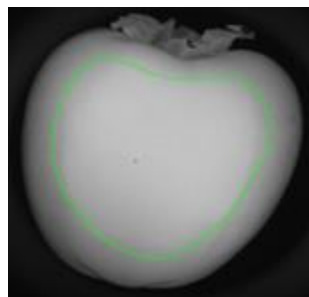

Figure 3. Hyperspectral image of a persimmon with the ROI selected.

3. Results and Discussion

3.1. Maturity classification

To know the stage of maturity of persimmon is essential because it may affect the duration of deastringency process, since the diffusion of CO_2 may be affected by the flesh firmness. According to Besada *et al.* (2010), a treatment of 24 h was effective to achieve a total removal of astringency at three different stages of maturity, but when CO_2 was applied for

less time, the effectiveness of the treatment depended on the initial stage of maturity of the fruit. At this point, maturity classification is necessary to guarantee adequate treatment duration. For this reason, several models using PLS-DA were built to classify the fruit in the three stage of maturity.

Table 1 shows the results obtained for the classification of persimmon fruit regarding to their stage of maturity using original spectra and SNV pre-processing, respectively. Both models achieved a similar rate of correct classification, although results of original spectra were a little better. It was possible because scatter problem was eliminated by selecting a central ROI in the image of the fruit. In both cases, samples of M2 were classified worse due to similarity to M3 and samples of M1 and M3 obtained the best percentage of correct classification. Despite obtaining good results with all wavelengths, hyperspectral systems are considered expensive and can capture a huge amount of information that is redundant and correlated, especially in contiguous wavelengths (Lorente *et al.,* 2012). Furthermore, current technology allows the configuration of multispectral cameras with up to five-seven CCD at a reasonable price. So, a selection of optimal wavelengths was conducted. To this end, the wavelengths with highest regression coefficients obtained in the PLS-DA model were selected as optimal for maturity classification.

Mohammadi *et al.* (2015) obtained similar results for classifying the maturity of persimmon fruits of a variety from Iran using RGB images. They obtained a relative correct classification of 89.2% using a large range of fruit of different maturities. On the other hand, Wei *et al.* (2014) used hyperspectral imaging and obtained a correct classification of 95.3% for 'Fangshi' persimmon using the spectra and the texture features of three wavelengths. Nevertheless, when they used only the spectra, the result was 85.9% of correct classification.

Table 1. Correct maturity classification (%) using PLS-DA with all and selected wavelengths from original spectra and pre-processed.

		All wavelengths				Selected wavelengths			
		M1	M2	M3	Total	M1	M2	M3	Total
Original	Calibration	94.1	84.8	93.9	90.9	91.2	84.8	93.9	90.0
	Classification	93.8	81.4	94.1	90.1	93.8	82.4	94.1	90.1
SNV	Calibration	97.1	84.8	93.9	91.9	94.1	84.8	93.9	90.9
	Classification	93.8	82.4	88.2	88.2	93.8	82.4	88.2	88.2

The average spectra of each stage of maturity and the optimal wavelengths are shown in Figure 4. These wavelengths were associated with different components of persimmon fruit: 570 and 590 nm provide information of carotenoids (Choudhary *et al.*, 2009; Merzlyak *et al.,* 2003), 680 nm, 710 nm and 730 nm of chlorophyll (Lleó et al., 2011; Rajkumar *et al.,* 2012) and 1000 nm of water content (Lu and Peng, 2006; Lleó *et al.,* 2011; Rajkumar *et al.,* 2012).
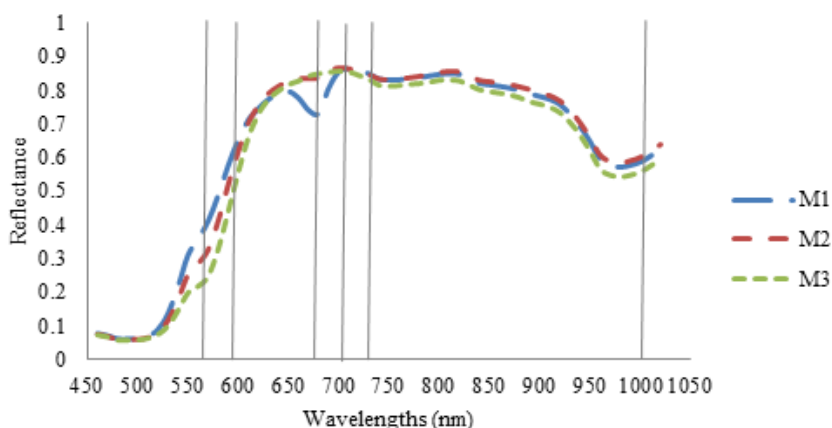

Figure 4. Average spectra of each maturity stage and the optimal wavelengths selected.

After generating the new PLS-DA models using only the optimal wavelengths, the percentage of classification obtained was similar to models using all wavelengths (Table 1). So it could be considered as a good result for a non-invasive, non-contact estimation technique with the advantage that the selected wavelengths fit into the sensitivity range of a standard CCD sensor.

3.2. Firmness prediction

Among the physiological changes related to fruit maturation, such as colour (Figure 1B) which is related to a

progressive accumulation of carotenoids during fruit maturation (Novillo *et al.,* 2016) or decline of soluble tannins (Salvador *et al.,* 2007), the change on fruit firmness is one of the most important to determine the optimum postharvest conditions. In this regard, Salvador et al., (2008) reported that fruit firmness can influence the effectiveness of the CO_2 treatment due to a loss of pulp structure associated to fruit softening may difficult the diffusion of CO_2. Therefore, apart from fruit maturity classification, the firmness parameter requires special attention. As seen in Figure 1, the firmness value decreased with the harvesting time (maturity), and therefore a model by PLS-R was built to predict the firmness of the previous classified fruits using only original spectra.

Figure 5 shows the results of the flesh firmness prediction, using all wavelengths and those selected for maturity classification. The high values of prediction were obtained using the six optimal wavelengths ($R^2 = 0.80$ and $SE_P = 4.34$ N) while using all of wavelengths was something worse ($R^2 = 0.77$ and $SE_P = 4.65$ N).

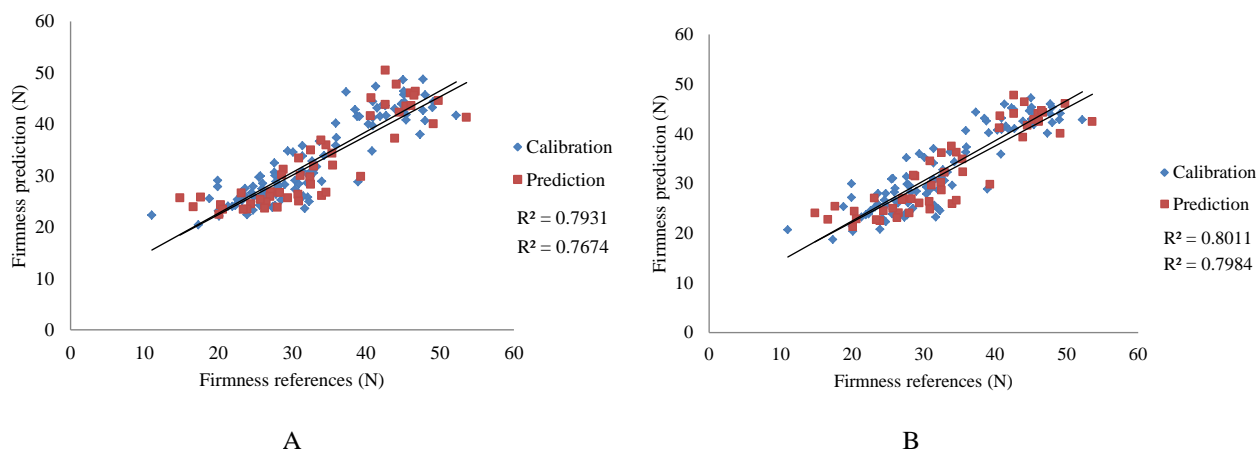A   B

Figure 5. Results of flesh firmness prediction using PLS-R. A) Prediction with all wavelengths; B) Prediction with only six optimal wavelengths.

But the results obtained were not as good as the prediction results of Wei *et al*. (2014) ($R^2 = 0.91$). It must be have into account that Wei *et al*. (2014) evaluated very different maturity stages, from unripe green fruits and overripe fruit; this implied marked different in firmness, since fruit is very firm when green and very soft at overripe. However, in the present study we evaluated three close maturity stages since the values of firmness were between 44 and 24N which implies that all the fruit showed crispy texture. On the contrary, in the present work, the firmness gave values from 47 N to 11 N which means that these fruits are apparently firm in all maturity stages, which is logical since it is treated to be consumed as firm and crispy fruit. Hence, for this fruit an 80% of prediction capability can be considered as a good achievement taking into account the little differences between classes, especially between classes M2 and M3. Moreover, in the case of 'Rojo Brillante' persimmon there is no minimum recommended degree of firmness, but values below 10 N following storage and marketing have been considered as unsuitable when commercializing crispy texture fruits (Salvador et al., 2007).

4. Conclusions

By means of hyperspectral imaging was possible to classify persimmon fruits according to their stage of maturity with a 90.1% of accuracy using PLS-DA. The maturity prediction was good despite analysing three close stages of maturity and using only six optimal wavelengths (570, 590, 680, 710, 730, 1000 nm).

Furthermore, an optimum prediction of flesh firmness using PLS-R and the optimal wavelengths was achieved ($R^2 = 0.80$), considering that all the fruit had commercial maturity and values of flesh firmness above 10 N.

Summarizing, this work demonstrates that hyperspectral imaging can be considered as a potential non-destructive tool to evaluate the maturity of 'Rojo Brillante' persimmon, helping in this way to decide the optimum conditions of some postharvest treatments.

Acknowledgements

References

Baranowski, P., W. Mazurek, J. Pastuszka-Wozniak, 2013. Supervised classification of bruised apples with respect to the time after bruising on the basis of hyperspectral imaging data. Postharvest Biology and Technology. 86, 249–258. Doi:10.1016/j.postharvbio.2013.07.005.

Besada, C., A. Salvador, L. Arnal, J.M. Martínez-Jávega, 2010. Optimization of the duration of deastringency treatment depending on persimmon maturity. Acta Horticulturae. 858, 69–74. Doi:10.17660/ActaHortic.2010.858.7.

Choudhary, R., T.J. Bowser, P. Weckler, N.O. Maness, W. McGlynn, 2009. Rapid estimation of lycopene concentration in watermelon and tomato puree by fiber optic visible reflectance spectroscopy. Postharvest Biology and Technology. 52, 103–109. Doi:10.1016/j.postharvbio.2008.10.002.

Gardner, J. L. 2007. Comparison of calibration methods for tristimulus colorimeters. Journal of Research of the National Institute of Standards. 112, 129–138.

Gaston, E., J.M. Frías, P.J. Cullen, C.P. O´Donnell, A.A. Gowen, 2010. Prediction of polyphenol oxidase activity using visible near-infrared hyperspectral imaging on mushroom (*Agaricusbisporus*) caps. Journal of Agricultural and Food Chemistry. 58, 6226–6233.

Gat, N. 2000.Imaging spectroscopy using tunable filters: A review.Technical report, Opto-Knowledge Systems Inc. OKSI.

Jiménez-Cuesta, M., J.M. Cuquerella, J.M. Martínez-Jávega, 1981. Proceedings International Society of Citriculture. 2, 750–753.

Lee, W.H., M.S. Kim, H. Lee, S.R. Delwiche, H. Bae, D.Y. Kim, B.K. Cho, 2014. Hyperspectral near-infrared imaging for the detection of physical damages of pear. Journal of Food Engineering. 130, 1–7. Doi:10.1016/j.jfoodeng.2013.12.032.

Lleó, L., J.M. Roger, A. Herrero-Langreo, B. Diezma-Iglesias, P. Barreiro, 2011. Comparison of multispectral indexes extracted from hyperspectral images for the assessment of fruit ripening. Journal of Food Engineering. 104, 612–620. Doi:10.1016/j.jfoodeng.2011.01.028.

Lorente D., N. Aleixos, J. Gómez-Sanchis, S. Cubero, O.L. García-Navarrete, J. Blasco, 2012. Recent advances and applications of hyperspectral imaging for fruit and vegetable quality assessment. Food Bioprocess Technology. 5, 1121–1142. Doi: 10.1007/s11947-011-0725-1.

Lu, R., Y. Peng, 2006. Hyperspectral scattering for assessing peach fruit firmness. Biosystems Engineering. 93, 161–171. Doi:10.1016/j.biosystemseng.2005.11.004.

Lü, Q., M. Tang, J. Cai, J. Zhao, S. Vittayapadung, 2011. Vis/NIR Hyperspectral imaging for detection of hidden bruises on kiwifruits. Czech Journal of Food Science. 29, 595–602.

Merzlyak, M.N., A.E. Solovchenko, A.A. Gitelson, 2003. Reflectance spectral features and non-destructive estimation of chlorophyll, carotenoid and anthocyanin content in apple fruit. Postharvest Biology and Technology. 27, 197–211. Doi:10.1016/S0925-5214(02)00066-2.

Mohammadi, V., K. Kheiralipour, M. Ghasemi-Varnamkhasti, 2015. Detecting maturity of persimmon fruit based on image processing technique. Scientia Horticulturae. 184, 123–128.

Novillo, P., A. Salvador, C. Crisosto, C. Besada, 2016. Influence of persimmon astringency type on physico-chemical changes from the green stage to commercial harvest. Scientia Horticulturae. 206, 7–14. Doi:10.1016/j.scienta.2016.04.030.

Rajkumar, P., N. Wang, G. EImasry, G.S.V. Raghavan, Y. Gariepy, 2012. Studies on banana fruit quality and maturity stages using hyperspectral imaging. Journal of Food Engineering. 108, 194–200. Doi:10.1016/j.jfoodeng.2011.05.002.

Salvador, A., L. Arnal, C. Besada, V. Larrea, A. Quiles, I. Pérez-Munuera, 2007. Physiological and structural changes during ripening and deastringency treatment of persimmon cv. 'RojoBrillante'. Postharvest Biol. Tec. 46, 181–188. Doi:10.1016/j.postharvbio.2007.05.003.

Salvador, A., L. Arnal, C. Besada, V. Larrea, I. Hernando, I. Perez-Munuera, 2008. Reduced effectiveness of the treatment for removing astringency in persimmon fruit when stored at 15 ℃. Physiological and microstructural study. Postharvest Biology and Technology. 49, 340-347. Doi:10.1016/j.postharvbio.2008.01.015.

Schmilovitch, Z., T. Ignat, V. Alchanatis, J. Gatker, V. Ostrovsky, J. Felföldi, 2014. Hyperspectral imaging of intact bell peppers. Biosystems Engineering. 117, 83-93. Doi:10.1016/j.biosystemseng.2013.07.003.

Teena, M.A., A. Manickavasagan, L. Ravikanth, D.S. Jayas, 2014. Near infrared (NIR) hyperspectral imaging to classify fungal infected date fruits. Journal of Stored Products Research. 59, 306-313. Doi:10.1016/j.jspr.2014.09.005.

Wei, X., F. Liu, Z. Qiu, Y. Shao, Y. He, 2014. Ripeness classification of astringent persimmon using Hyperspectral Imaging technique. Food Bioprocess Technology. 7, 1371–1380. Doi: 10.1007/s11947-013-1164-y.

Yang, C.C., M.S. Kim, S. Kang, B.K. Cho, K. Chao, A.M. Lefcourt, D.E. Chan, 2012. Red to far-red multispectral fluorescence image fusion for detection of fecal contamination on apples. Journal of Food Engineering. 108, 312–319. Doi:10.1016/j.jfoodeng.2011.08.008.

Zhang, B., J. Li, S. Fan, W. Huang, C. Zhao, C. Liu, D. Huang, 2015. Hyperspectral imaging combined with multivariate analysis and band math for detection of common defects on peaches (Prunuspersica). Computers and Electronics in Agriculture. 114, 14–2. Doi:10.1016/j.compag.2015.03.015.